NANOSYSTEMS:
PHYSICS, CHEMISTRY, MATHEMATICS

L. Rohmawati, et al. *Nanosystems: Phys. Chem. Math.*, 2022, **13** (6), 640–648.
http://nanojournal.ifmo.ru
DOI 10.17586/2220-8054-2022-13-6-640-648

Original article

The characteristics of TiO_2 anatase from tulungagung sand as an antibacterial material

L. Rohmawati[1], Istiqomah[2], A. A. Pratama[1], W. Setyarsih[1], N. P. Putri[1], Munasir[1], Darminto[3]

[1]Physics Department, Faculty of Mathematics and Natural Science, Universitas Negeri Surabaya, Ketintang, Gayungan, Surabaya 60231, Indonesia

[2]Physics Department, Faculty of Mathematics and Natural Science, Universitas Negeri Malang, Semarang 5, Malang 65145, Indonesia

[3]Physics Department, Faculty of Science and Data Analytics, Institut Teknologi Sepuluh Nopember (ITS), Keputih, Sukolilo, Surabaya 60111, Indonesia

Corresponding author: L. Rohmawati, lydiarohmawati@unesa.ac.id

ABSTRACT TiO_2 anatase is a material that has good photocatalytic properties. The synthesis of TiO_2 anatase from Tulungagung natural sand used the leaching method. The synthesized samples were characterized by TGA, XRD, FTIR, BET, SEM, UV-DRS and tested for antibacterial effect. In this study, the TiO_2 anatase phase was already formed and experiencing three stages of weight loss. It had stretching vibration of the OH group, had a bending mode of water Ti–OH, and Ti–O–Ti at wavenumbers 4000 to 400 cm^{-1}. It also had a mesoporous size, was spherical with a grain size of 58 nm and had an energy gap of 3.42 eV. TiO_2 anatase with a 600 μg/mL concentration could reduce Escherichia coli, Staphylococcus aureus, and Pseudomonas aeruginosa bacteria. Therefore, TiO_2 anatase has the potential in an antibacterial agent.

KEYWORDS TiO_2 anatase, natural sand, antibacterial

FOR CITATION Rohmawati L., Istiqomah, Pratama A.A., Setyarsih W., Putri N.P., Munasir, Darminto The characteristics of TiO_2 anatase from tulungagung sand as an antibacterial material. *Nanosystems: Phys. Chem. Math.*, 2022, **13** (6), 640–648.

1. Introduction

The rapid development of nanotechnology has increased the number of nanoparticle-based materials. Due to their unique physical properties, nanomaterials have changed their functions in commercial product applications, including food packaging, drug delivery, biosensors and antibacterial agents [1]. One of them is titanium dioxide (TiO_2) nanomaterial, widely studied in the last two decades [2]. TiO_2 nanoparticles are considered as an option in biological and environmental remediation applications compared to other semiconductor materials. TiO_2 is available in nature, low cost, and non-toxic, has high surface area and has unique physiochemical properties. In addition, this material has also photocatalytic activity, biocompatibility and reasonable thermal stability [3]. TiO_2 anatase has a tetragonal structure and is formed at lower temperatures [4]. Anatase has the best photocatalytic properties among the three phases than rutile and brookite [5]. Research of TiO_2 in antibacterial agents has been ongoing for the past 20 years. Antibacterial refers to substances that do away or obstruct the growth of microorganisms [6]. Although gram-positive bacteria can form spores and are difficult to inactivate, TiO_2 with photocatalytic properties can kill gram-positive and gram-negative bacteria [7]. The antibacterial effect of TiO_2 plays an essential role in the medical world because it can kill pathogenic bacteria, such as Escherichia coli, Staphylococcus aureus and Pseudomonas aeruginosa [8]. The antibacterial properties of TiO_2 depend on the size of particles and concentration of particles, thus affecting the length of retention time of bacteria [9, 10]. Indonesia, especially the Tulungagung region in East Java, has a natural wealth of mineral sand, where the main content in mineral sand is Fe and Ti elements, which are bound to other elements. The elements of Fe and Ti bind to each other to form ilmenite ($FeTiO_3$), hematite (Fe_2O_3) and magnetite (Fe_3O_4) compounds [11]. One is the ilmenite compound of the three compounds extracted into titanium dioxide (TiO_2) [12]. The anatase compound (TiO_2) obtained from the extraction of ilmenite ($FeTiO_3$) is a content of coastal sand that can be used as an antibacterial agent [13].

Several researchers have extracted TiO_2 from the Ilmenite sands of the Indonesian island of Bangka with specific methods. Lalasari et al. [14] synthesized TiO_2 using the hydrothermal method using NaOH, but as for the results of their research, there were two phases, namely rutile TiO_2 and ilmenite ($FeTiO_3$). Aristanti et al. [15] reported that TiO_2 could be synthesized using a caustic fusion process using NaOH and a leaching process with H_2SO_4. As a result, he produced anatase and rutile phases of TiO_2 with impurities in the form of α-Fe_2O_3. Likewise, in Wahyuningsih et al.'s research [16], anatase TiO_2 can be synthesized using a dissolution roasted ilmenite process with Na_2S followed by a leaching process with H_2SO_4. The roasted ilmenite process requires a high temperature of 900 °C for 6 hours. Supriyatna et al. [17] also carried out the same process, but the leaching process used HCl solvent, and the products obtained were rutile TiO_2 (94.6 %) and ilmenite impurities.

Each sand in Indonesia has different characteristics, such as in the Tulungagung area, where it is known that the TiO_2 and Fe_2O_3 contents in the Tulungagung mineral sand are 12.2 and 83.35 %, correspondingly [13]. So far, Tulungagung sand has only been used as a building material, and there has been no further use. Thus, to increase the usefulness of Tulungagung sand, innovation is needed to explore the sand's content. As explained above, TiO_2 can be applied as an antibacterial material. Based on the literacy results from previous studies, the antibacterial characteristics of the anatase TiO_2 compound from Tulungagung sand have never been reported. The novelty of this research is the analysis of the antibacterial aspect of TiO_2 anatase from Tulungagung sand. In addition, anatase TiO_2 nanoparticles were synthesized using the leaching method with the chemical solvent 8 M H_2SO_4 and low temperature in this study. High concentrations of sulfuric acid in the leaching process can produce TiO_2 anatase [16]. In this study, Tulungagung mineral sand was not roasted like some of the studies above but was carried out with a simple method, namely taking ilmenite sand from the Tulungagung sand using a magnetic rod carried out by the leaching process. Therefore, the results expect that TiO_2 anatase from these natural ingredients can be excellent antibacterial material.

2. Materials and method

2.1. Materials

The materials needed in this research include mineral sand in Tulungagung, East Java, Indonesia, H_2SO_4 (Sigma Aldrich 99 %), and demineralized water. Equipment needed for the synthesis process includes bar magnet, mortar pestle, 200 mesh sieve, vacuum pump, hot plate stirrer, pH meter, glass beaker, and furnace.

2.2. Experimental methods and data analysis

In the first stage, Tulungagung mineral sand was washed first and dried. The next stage was to separate magnetic and non-magnetic sand using a magnetic rod. After that, the magnetic sand is sieved using a 200 mesh strainer to obtain a fine homogeneous powder. Next was the leaching process, where the powder was dissolved with H_2SO_4 8 M and heated using a hot plate stirrer at a temperature of 110 °C for 30 minutes until it formed a slurry solution. After that, it was vacuum pumped to separate the $TiOSO_4$ filtrate and $FeSO_4$ precipitate, with reaction presented below:

$$\mathrm{FeTiO_{3(s)} + 2H_2SO_{4(aq)} \longrightarrow FeSO_{4(s)} + TiOSO_{4(aq)} + 2H_2O_{(l)}}. \tag{1}$$

$TiOSO_4$ filtrate was added with distilled water and heated using a hot plate stirrer at 100 °C until forming sediment, with the following hydrolysis reaction:

$$\mathrm{TiOSO_{4(aq)} + 2H_2O_{(l)} \longrightarrow TiO(OH)_{2(s)} + H_2SO_{4(aq)}}. \tag{2}$$

Furthermore, the sediment was washed with demineralized water to obtain a pH of 7, then filtered and calcined at 600 °C during 2 hours, with condensation reaction as:

$$\mathrm{TiO(OH)_{2(s)} \longrightarrow TiO_{2(s)} + H_2O_{(l)}}. \tag{3}$$

The calcined samples were then characterized by TGA, XRD, FTIR, BET, SEM, UV-DRS, and antibacterial activity test. Thermo Gravimetric Analyzer (TGA) Linseis model STA PT 1000 was used to observe the mass change from the sample thermal decomposition. The phase identification of the sample used data from X-ray Diffraction (XRD) type Phillips X'Pert MPD (multi-purpose diffraction) with monochromatic wavelength CuKα, voltage 40 kV/40 mA and scattering angle of 10 to 90°. The data from the XRD were analyzed qualitatively using the QualX Software. The sample's Ti–O–Ti, Ti–OH, and OH functional groups could be identified by characterization using the Fourier transform infrared (FTIR) brand Shimadzu type IRPrestige 21 with 4000 – 400 cm^{-1} of wavenumber. The data obtained from the Brunauer–Emmett–Teller (BET) characterization of Quantrachome TouchWin 1.2 type were analyzed using the Barret–Joyner–Halenda (BJH) method to determine the sample pore size and surface area. Characterization Scanning Electron Microscopy (SEM), the Inspect-S50 type FEO, operated at 20 kV, 60 A, magnifying 150,000 times equipped with EDX (Energy Dispersive X-ray), was used to observe the samples' morphology. The grain diameter distribution in the sample was analyzed using ImageJ software. The Ultra Violet-Visible Diffuse Reflectance Spectroscopic (UV-Vis DRS) characterization of the Analytical Jena type Specord 200 Plus was carried out to observe the UV-visible absorbance spectrum in samples with 190 – 800 nm of wavelength. The data from UV-DRS could also be identified as the sample bandgap using Tauc plot analysis.

2.3. Preparation of antibacterial test

Antibacterial testing on samples was carried out using the International Normative ASTM E2149-10 standard on gram-positive (Staphylococcus aureus) and gram-negative (Escherichia coli and Pseudomonas aeruginosa) bacteria. The first stage was to perform cell culture of each bacterium in a stationary phase and measure it using a spectrometer of 600 nm. After that, it was stored in liquid medium and incubated at 37 °C until it reached bacterial concentration 108 CFU/mL. To obtain the concentration of bacteria about 105 CFU/mL, it was carried out three times dilute from 1/10. In the second stage, sample TiO_2 powder was dissolved with water demineralized until it formed suspension. The sample TiO_2 with concentrations of 100, 200, 300, 400, 500, and 600 μg/mL were each given a bacterial solution with a

105 CFU/mL concentration and irradiated using a UVA lamp for 3 hours. Then each 10 μL of the test solution was grown in a petri dish at 37 °C for 24 hours, and observations were made.

3. Results and discussion

3.1. Thermo gravimetric analysis (TGA)

Thermogravimetric analysis allows one to study the magnitude of the reduction in sample weight due to thermal treatment, with the test starting at room temperature up to 850 °C. Based on the TGA curve (Fig. 1), one concludes that there were three stages of sample weight loss with increasing temperature, and significant weight loss occurred at temperatures less than 580 °C. After 580 °C, the thermogravimetric curve was almost flat, indicating that the sample did not lose weight up to 680 °C. The sample weight loss was easier to observe using a weight derivative of thermogravimetric curve. In the first stage, the sample lost weight at a temperature of 200 to 330 °C by 8.1 % because the absorbed water was dehydrated. At a temperature of 330 to 580 °C in the second stage, the sample experienced a weight loss of 10.53 % due to the decomposition of hydroxyl compounds and changes due to the crystallization process from the amorphous phase to anatase transformation. The product was utterly transformed into the anatase TiO_2 phase at 580 °C. The same observation at this temperature had also been reported by Zablotsky et al. [18] where TiO_2 anatase was fully formed at 560 °C. There was no weight loss at a temperature of 580 to 640 °C, so there was no phase change. The third stage was a phase change from the anatase to rutile phase at 680 to 810 °C followed by 9.5 % sample weight loss because of removal of impurity. At last, at the temperature of 810 until 850 °C, the curve was almost flat.

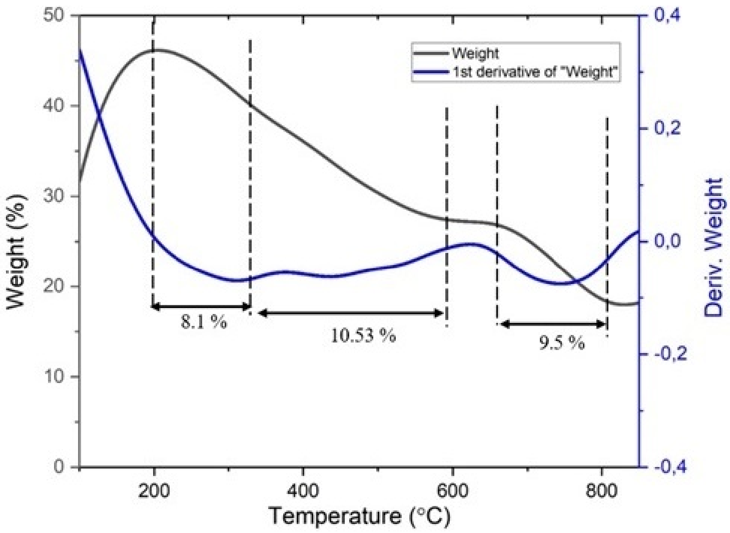

FIG. 1. TGA and the first derivative weight of sample

3.2. X-ray diffraction (XRD)

The diffraction pattern of the synthesized sample is shown in Fig. 2. The data obtained from XRD were analyzed using QualX software to identify the TiO_2 anatase phase. The diffractogram in Fig. 2 shows that the anatase phase TiO_2 has been completely formed in the sample. The anatase phase is formed at a diffraction angle of 25.35°. It is the highest diffraction intensity with crystal orientation (101). Other diffraction peaks which show the anatase phase is 37.03, 37.86, 38.6, 48.11, 53.94, 55.09, 62.13, 62.76, 68.80, 70.32, 75.08, 75.35, and 82.73 ° with miller indices (013), (004), (112), (200), (105), (211), (213), (204), (116), (220), (215), (301), and (224), which are appropriate with Joint Committee on Powder Diffraction Standard (JCPDS) data number 9015929. The results are similar to those reported by several researchers [19–21].

3.3. Fourier transform infrared (FTIR)

The chemical bonding functional group of a sample can be determined by FTIR characterization. This characterization was carried out using infrared spectroscopy in the wavenumber of 4000 – 400 cm^{-1}. The results of the FTIR characterization can be seen in Fig. 3. In this study, the synthesized samples had absorption peaks at wave numbers of 3423.76, 1641.48, 1087.89, 669.32, 551.15 cm^{-1}. Firm absorption peaks at wave numbers 551.15 and 669.32 cm^{-1} indicated Ti–O–Ti bonds in the TiO_2 lattice and were characteristic of TiO_2 anatase [21]. Al-Taweel and Saud [22] also observed this type of bond and Dicastillo et al. [23], namely, the absorption peak occurred at 700 – 400 cm^{-1} of wavenumber. The absorption peak at a wavenumber of 1087.89 cm^{-1} was a stretching or deviational vibration of the Ti–O–Ti bond in TiO_2 [24]. The peak of 1641.48 cm^{-1} showed a bending mode of water Ti–OH which indicated the presence of some

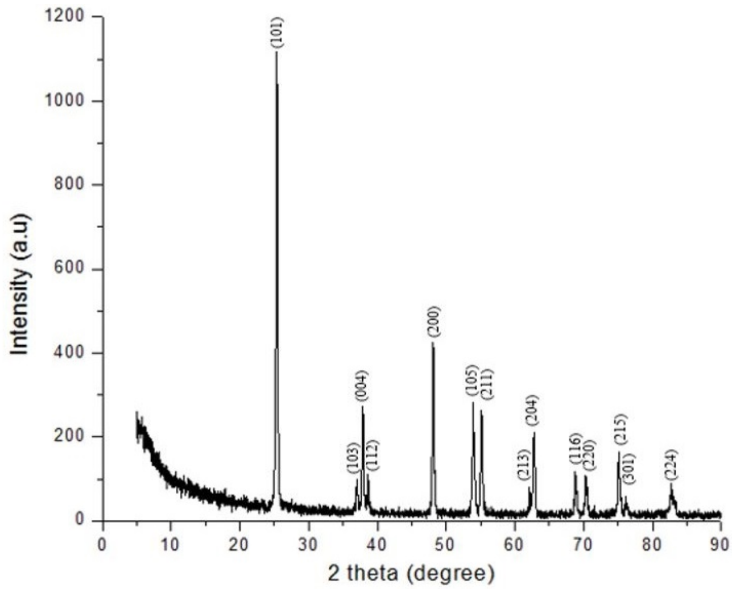

FIG. 2. XRD pattern of sample

H_2O [23, 25] and was a type of scissors deformation of adsorbed water protonation [26, 27]. The functional groups at 3423.76 cm^{-1} of wavenumber indicated stretching vibration of the OH group [23] and adsorbed water molecules [28]. The same results were also observed by several researchers, Al-Taweel and Saud [22], who reported that the absorption peak at 3600 – 3400 cm^{-1} indicated an intermolecular connection in the hydroxyl group for water molecules with TiO_2 surfaces. The functional group hydroxyl group had an essential role in the microbicidal mechanism [29, 30].

3.4. Brunauer–Emmett–Teller (BET)

Pore size, pore structure and pore surface area in the sample can be investigated using BET characterization. Fig. 4 shows that the isotherm curve forms a hysteresis loop in the relative pressure range (0.9 – 1.0 P/P_0). The TiO_2 isotherm curve formed belongs to the V type with the H_1 type hysteresis loop in the form of a cylindrical pore, which shows the characteristics of mesoporous materials [31]. The adsorption-desorption isotherm curve has an open end, wherein the adsorption process nitrogen gas will be absorbed and enter the pores; thus, the volume of nitrogen gas absorbed will be greater than that released. When used as antibacterial material, it has the potential to inhibit bacteria well. Several researchers have revealed that the mesoporous material in TiO_2 is very efficient as an antimicrobial agent [32, 33].

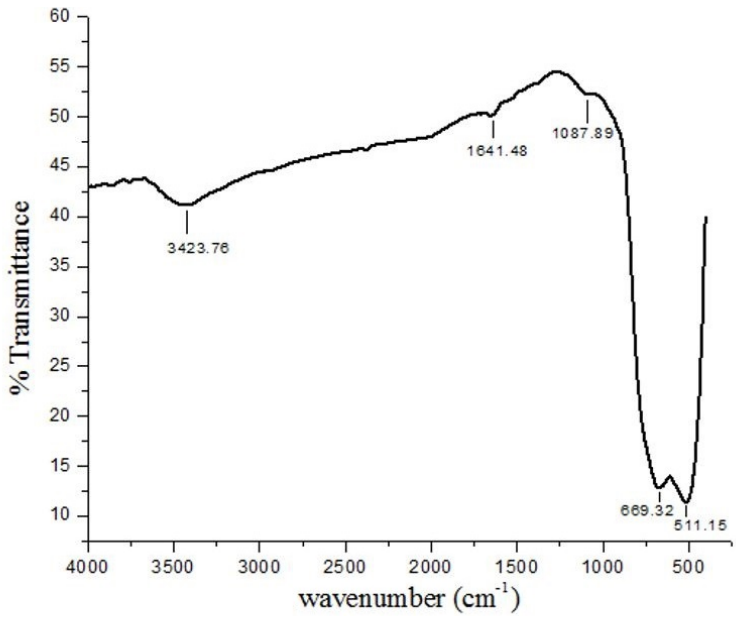

FIG. 3. FTIR spectra of sample

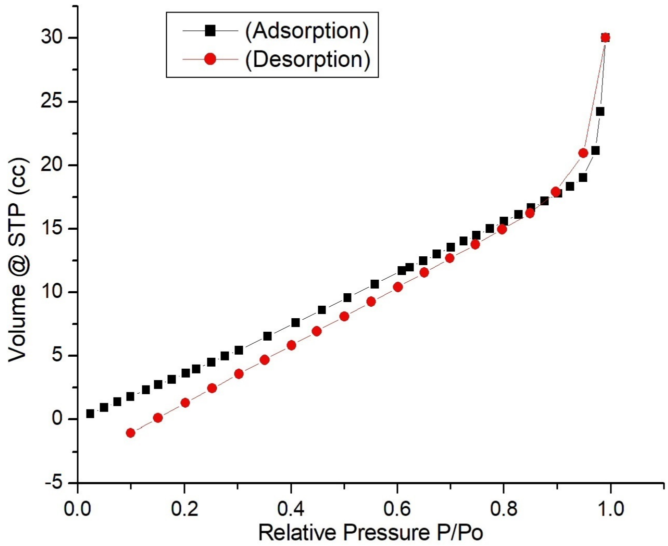

FIG. 4. The isotherms of sample

Based on the analysis of Barret Joyner Hallenda (BJH), it is known that the pore size distribution of the synthesized sample from the desorption curve (Fig. 5) is 3.06 nm (pore radius 15.31 Å). The size belongs to the mesoporous category (2 nm $< d <$ 50 nm). The BET analysis represents that the TiO_2 sample had 727,590 m^2/g of surface area. This value is greater than the results of several researchers, including 266 m^2/g [33], 65.65 m^2/g [34], 124 m^2/g [35]. The large pore surface area possessed by the synthesized TiO_2 sample can be the main determining factor in increasing antimicrobial activity because it provides good contact between nanoparticles and microorganisms [36].

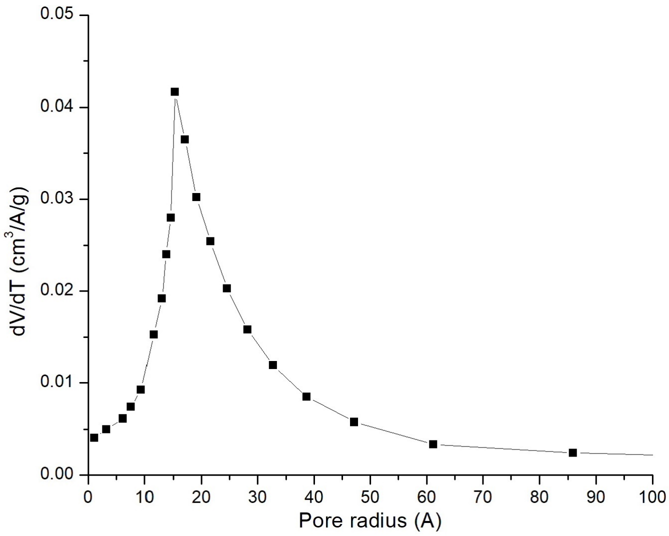

FIG. 5. Desorption curve on the sample

3.5. Scanning electron microscopy (SEM)

Figure 6 depicts the surface morphology of the anatase TiO_2 sample. The figure shows that the sample's morphology is spherical, although there is still agglomeration at some points. Based on the Energy Dispersive X-ray (EDX) results, 100 % anatase TiO_2 samples were formed from Ti and O elements without any other elements.

Analysis of the grain size distribution of the anatase TiO_2 sample using ImageJ software, the results of which are shown in Fig. 7. The grain size of the anatase TiO_2 sample is 58 nm, which results from considering about 100 grains, indicating a size smaller than 100 nm, and includes nanoparticles.

3.6. Ultra violet-visible diffuse reflectance spectroscopic analysis (UV-Vis DRS)

The absorbance of the sample at a specific wavelength of light can be determined using UV-DRS analysis. In Fig. 8(a), it appears that the sample has a strong UV absorption with a wavelength of less than 400 nm. However, at a wavelength

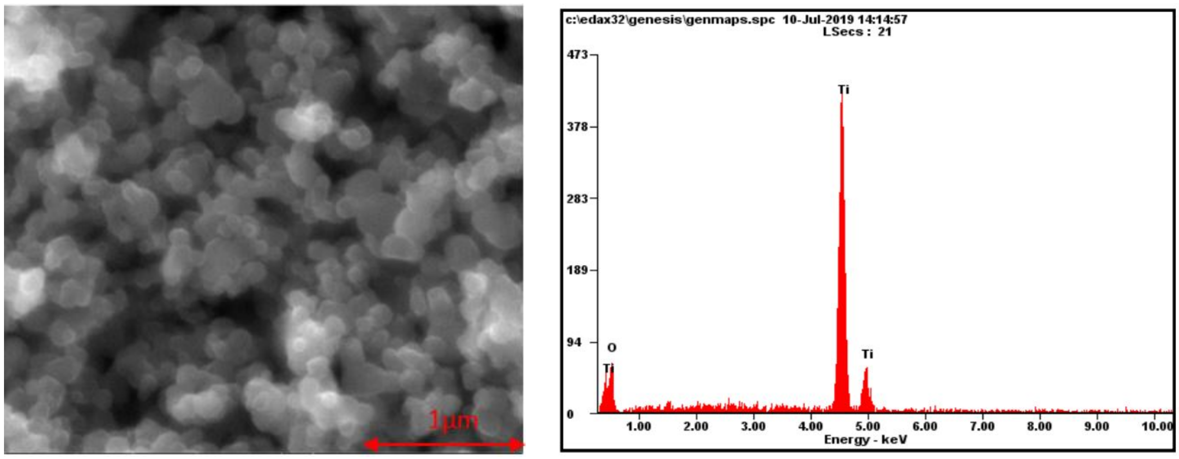

(a) (b)

FIG. 6. Characterization results (a) SEM (b) EDX on samples

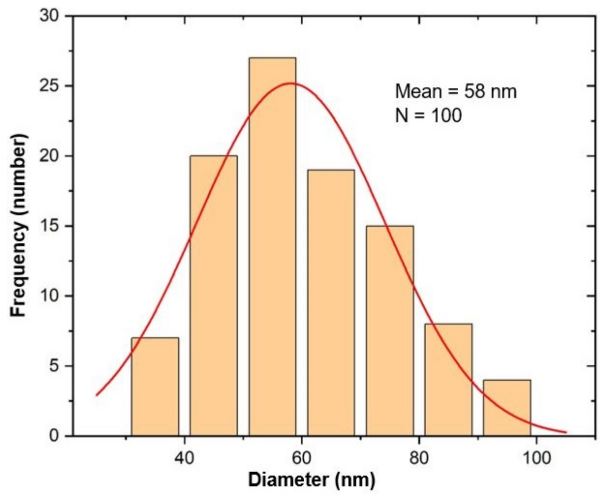

FIG. 7. Distribution of sample grain sizes from SEM image

in visible light, no absorption is observed by the sample in this region. It means that the photon energy at that wavelength does not stimulate electrons to move to a higher energy level [37]. The energy gap of the sample can be determined using the Tauc plot analysis, the results of which can be seen in Fig. 8(b). The sample has an energy gap of 3.42 eV and includes TiO_2 anatase [38, 39].

3.7. Antibacterial behaviour

In this study, the bacteria used were *E. coli*, *E. aureus*, and *P. aeruginosa*, with concentrations of TiO_2 200, 300, 400, 500, and 600 μg/ml. Table 1 displays the antibacterial behaviour of TiO_2 with several cell concentrations and log reduction. Bacteria dissolved in demineralized water without UV radiation were used as a control. When irradiated with UV light, TiO_2 showed antibacterial activity characterized by wane in the number of bacteria as the concentration of TiO_2 increased. It shows that UV radiation can obstruct the growth of bacteria. The 600 μg/mL concentration of TiO_2 has the highest inhibitory ability for both gram-positive and gram-negative bacteria which is characterized by the number of live bacteria around $3.7 \cdot 10^3$ CFU/mL. At concentrations of 400 to 600 μg/mL, it was found that there was a slight decrease in the number of live bacterial colonies for *E. coli*, *S. aureus*, and *P. aeruginosa* bacteria, as shown in Fig. 9, where it was inhibited the number of bacterial growth although slowly. It is because the dilution factor affects the diffusion process, where a high concentration of TiO_2 allows low solubility, causing limited diffusion rates. It influences the ability of TiO_2 to inhibit the growth of bacteria such as *E. coli*, *S. aureus*, and *P. aeruginosa*. Valgas et al. [40] stated that the deposition of antibacterial compounds could cause a limited diffusion rate. This study was limited to a concentration of 600 μg/mL. It is because the data at that concentration is already sufficient to show the ability of TiO_2 as an antibacterial in both gram-positive and gram-negative bacteria.

The antibacterial behaviour of TiO_2 can be explained by an oxidation reaction when exposed to UV radiation [41]. TiO_2 surface exposed to UV radiation will produce hydroxyl and superoxide, reactive oxygen species (ROS). The surface

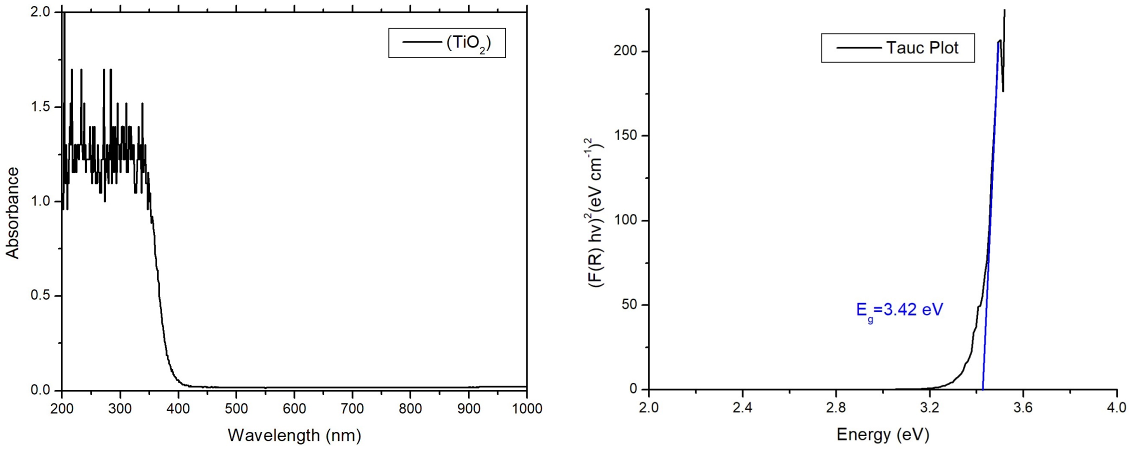

(a) (b)

FIG. 8. (a) Uv-vis spectra of sample, (b) UV-Tauc plot of sample

TABLE 1. Antibacterial behaviour of TiO_2 at different concentrations

Bacteria	*Escherichia coli*		*Staphylococcus aureus*		*Pseudomonas aeruginosa*	
TiO_2 (μg/mL)	Cell conc. (CFU/mL)	Log Reduction	Cell conc. (CFU/mL)	Log Reduction	Cell conc. (CFU/mL)	Log Reduction
0	$2.6 \cdot 10^5$	5.41 ± 0.03	$3.4 \cdot 10^5$	5.54 ± 0.04	$2.6 \cdot 10^5$	5.41 ± 0.11
200	$4.0 \cdot 10^4$	4.60 ± 0.02	$4.3 \cdot 10^4$	4.63 ± 0.09	$2.8 \cdot 10^4$	4.44 ± 0.15
300	$3.3 \cdot 10^4$	4.51 ± 0.05	$2.9 \cdot 10^4$	4.46 ± 0.02	$2.1 \cdot 10^4$	4.32 ± 0.12
400	$4.5 \cdot 10^3$	3.65 ± 0.11	$3.8 \cdot 10^3$	3.57 ± 0.04	$2.1 \cdot 10^3$	3.32 ± 0.08
500	$4.1 \cdot 10^3$	3.61 ± 0.09	$3.2 \cdot 10^3$	3.50 ± 0.03	$1.8 \cdot 10^2$	2.25 ± 0.06
600	$3.7 \cdot 10^3$	3.50 ± 0.07	$3.4 \cdot 10^2$	2.53 ± 0.03	$1.2 \cdot 10^2$	2.07 ± 0.09

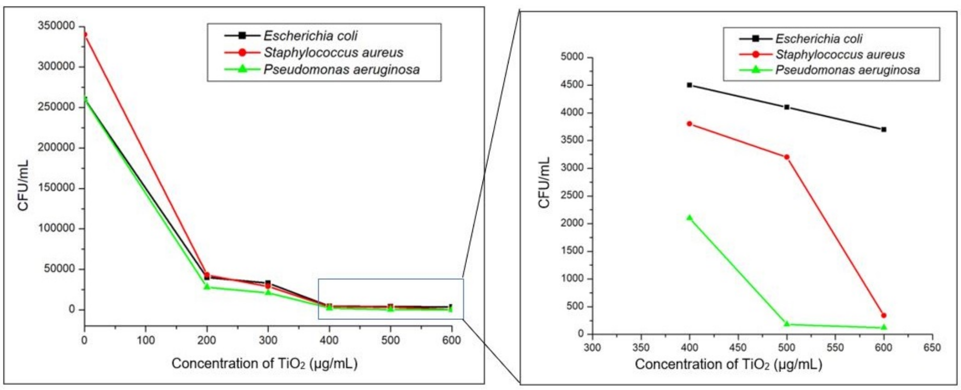

FIG. 9. Antibacterial activity with the concentration of TiO_2

of the bacteria will come into contact with TiO_2 particles, which are oxidized when exposed to UV radiation. Makowski and Wardas [42] stated that the generation of reactive oxygen compounds could destroy bacteria through damage to bacterial cell walls. Observation of the TiO_2 antibacterial activity for 24 hours showed that TiO_2 was effective in obstructing the accretion of *S. aureus*, *P. aeruginosa*, and *E. coli*. The antibacterial activity of *S. aureus* and *P. aeruginosa* as gram-positive bacteria was higher than that of *E. coli* as gram-negative bacteria. It is because the three bacteria have different cell wall structures and thicknesses [41]. Cell wall helpfulness is to protect bacteria from antibacterial compounds that can enter and kill bacteria. The cell wall structure of gram-negative bacteria is more complex and has a layer of peptidoglycan, and a layer of lipopolysaccharide, which acts as a barrier to the entry of antibacterial compounds into bacterial cells. Gram-negative bacteria are more resistant to antibacterial from TiO_2 when compared to gram-positive bacteria.

In contrast, gram-positive bacteria have no lipopolysaccharide layer, allowing antibacterial compounds to enter the cell and cause lysis. The single-layered gram-positive cell wall structure is relatively simple, making it easier for antibacterial compounds to enter cells and inhibit bacterial growth. In addition to cell wall thickness, the duration of UV radiation also affects the antibacterial activity of TiO_2. TiO_2 concentration of 600 μg/mL was able to reduce bacteria *E. coli*, *S. aureus* and *P. aeruginosa*, respectively $3.7 \cdot 10^3$; $3.4 \cdot 10^2$ and $1.2 \cdot 10^2$ CFU/mL. The longer the UV radiation, the more ROS produced and can obstruct the growth of more bacteria. The size of TiO_2 nanoparticles also inhibited bacterial growth [39].

4. Conclusion

TiO_2 anatase has been successfully synthesized from mineral sands of Tulungagung using the hydrothermal leaching method in this study. The characteristics of TiO_2 anatase can be seen from the results of XRD, TGA, FTIR, BET, SEM, UV-DRS, and antibacterial tests on *E. coli*, *S. aureus*, and *P. aeruginosa* bacteria. The results of the characterization include: TiO_2 anatase phase has been formed, has 3 stages of weight loss, has Ti–O–Ti, Ti–OH, and OH functional groups. It also had a pore size of 3.06 nm with a surface area of 727.590 m^2/g and mesoporous category. The synthesized TiO_2 had a spherical morphology with a grain size of 58 nm. TiO_2 had strong absorption of UV light with a wavelength of less than 400 nm and had an energy gap of 3.42 eV. TiO_2 with a 600 g/mL concentration had the most optimum reducing ability on *E. coli*, *S. aureus* and *P. aeruginosa* bacteria, respectively $3.7 \cdot 10^3$; $3.4 \cdot 10^2$ and $1.2 \cdot 10^2$ CFU/mL for 24 hours.

References

[1] Lu P., Huang S., Chen Y., Chiueh L., Shih D.Y. Analysis of Titanium Dioxide and Zinc Oxide Nanoparticles in Cosmetics. *J. Food Drug Anal.*, 2015, **23** (3), P. 587–594.

[2] Hayle S.T. Synthesis and Characterization of Titanium Oxide Nanomaterials Using Sol-Gel Method. *J. Nanosci. Nanotechnol.*, 2014, **2** (1), P. 1–7.

[3] Khashan K.S., Sulaiman G.M., Abdulameer F.A., Albukhaty S., Ibrahim M.A., Al-Muhimeed T., Alobaid A.A. Antibacterial Activity of TiO_2 Nanoparticles Prepared by One-Step Laser Ablation in Liquid. *Appl. Sci.*, 2021, **11** (4623): P. 2–12.

[4] Al-Dhahir T.A. Quantitative Phase Analysis for Titanium Dioxide from X-ray Powder Diffraction Data Using the Rietveld Method. *Diyala J. for Pure Science*, 2013, **9** (2), P. 108–119.

[5] Luís A.M., Neves M.C., Mendonça M.H., Monteiro O.C. Influence of Calcination Parameters on The TiO_2 Photocatalytic Properties. *Mater. Chem. Phys.*, 2011, **125** (2), P. 20–25.

[6] Piskin S., Palantöken A., Yilmaz M.S. Antimicrobial Activity of Synthesized TiO_2 Nanoparticles. *Int. Conf. on Emerging Trends in Engineering and Technology (ICETET'2013)*. Patong Beach, Dec. 7–8, Phuket (Thailand), 2013.

[7] Kongsong P., Sikong L., Niyomwas S., Rachpech V. Photocatalytic Antibacterial Performance of Glass Fibers Thin Film Coated with N-Doped SnO_2/TiO_2. *Sci. World J.*, 2014, 869706.

[8] Mahdy S.A., Mohammed W.H., Kareem H.A. The Antibacterial Activity of TiO_2 Nanoparticles. *J. Univ. Babylon*, 2017, **25** (3), P. 955–961.

[9] Sánchez-López E., Gomes D., Esteruelas G., Bonilla L., Lopez-Machado A.L., Cano A., Espina M., Ettecheto M., Camins A., Silva A.M. Metal-based nanopraticles as antimicrobial agents: An overview. *Nanomaterials*, 2020, **10** (2), 292.

[10] Han C., Lalley J., Namboodiri D., Cromer K., Nadagouda M.N. Titanium dioxide-based antibacterial surfaces for water treatment. *Curr. Opin. Chem. Eng.*, 2016, **11**, P. 46–51.

[11] Setiawati L.D., Rahman T.P., Nugroho D.W., Nofrizal, Ikono R., Suryandaru, Yuswono, Siswanto, Rochman N.T. Ekstraksi Titanium Dioksida (TiO_2) Dari Pasir Besi Dengan Metode Hidrometalurgi. *Proceeding Seminar Semirata FMIPA*, 2013, **1** (1), P. 465–468.

[12] Mahdi E.M., Shukor M.H.A., Yusoff M.M.S., Wilfred P. XRD and EDXRF analysis of anatase Nano-TiO_2 synthesized from mineral precursors. *Adv. Mat. Res.*, 2013, **620**, P. 179–185.

[13] Istiqomah, Putri A.N., Patmawati T., Rohmawati L., Setyarsih, W. Ekstraksi Titanium Dioksida (TiO_2) Anatase Menggunakan Metode Leaching dari Pasir Mineral Tulungagung. *Akta Kimia Indonesia*, 2019, **4** (2), P. 145–151.

[14] Lalasari L.H., Firdiyono F., Yuwono A.H., Harjanto S., Suharno. Preparation, Decomposition and Characterizations of Bangka-Indonesia Ilmenite ($FeTiO_3$) derived by Hydrothermal Method using Concentrated NaOH Solution. *Adv. Mat. Res.*, 2012, **535–537**, P. 750–756.

[15] Aristanti Y., Supriyatna Y.I., Masduki N.P., Soepriyanto S. Effect of calcination temperature on the characteristics of TiO_2 synthesized from ilmenite and its applications for photocatalysis. *IOP Conf. Ser.: Mater. Sci. Eng.*, 2019, **478**, P. 1–8.

[16] Wahyuningsih S., Ramelan A.H., Pramono E., Sulistya A.D., Argawan P.R., Dharmawan F.D. Synthesis of Anatase and Rutile TiO_2 Nanostructures from Natural Ilmenite. *AIP Conf. Proc.*, 2016, 1710.

[17] Supriyatna Y.I., Astuti W., Sumardi S., Sudibyo, Prasetya A., Ginting L.I.B., Irmawati Y., Asri N.S., Bayu H.T., Petrus M. Correlation of Nano Titanium Dioxide Synthesis and the Mineralogical Characterization of Ilmenite Ore as Raw Material. *Int. J. Technol.*, 2021, **12** (4), P. 749–759.

[18] Zablotsky D., Maiorov M.A., Krumina A., Romanova M., Blums E. Role of precursor composition in the polymorph transformations, morphology control and ferromagnetic properties of nanosized TiO_2. *Condensed Matter – Materials Science*, 2021, arXiv:2102.03058.

[19] Suliman A.A.M., Isha R., Seman M.N.A., Ahmad A.A., Roslan J. Mesoporous Ce-doped Ti: Ash Photocatalyst Investigation in Visible Light Photocatalytic Water Pretreatment Process. *Bull. Chem. React. Eng. Catal.*, 2020, **15** (2), P. 367–378.

[20] Johari N.D., Rosli Z.M., Juoi J. M., Yazid S.A. Comparison on the TiO_2 crystalline phases deposited via dip and spin coating using green sol-gel route. *J. Mater. Res. Technol.*, 2019, **8** (2), P. 2350–2358.

[21] Bagheri S., Shameli K., Hamid S.B.A. Synthesis and Characterization of Anatase Titanium Dioxide Nanoparticles Using Egg White Solution via Sol-Gel Method. *J. Chem.*, 2013, **2013**.

[22] Al-Taweel S.S., Saud H.R. New route for synthesis of pure anatase TiO_2 nanoparticles via ultrasound assisted sol-gel method. *J. Chem. Pharm. Res.*, 2016, **8** (2), P. 620–626.

[23] Dicastillo, Patiño C., Palma J.L., Alburquenque D., Escrig J. Novel Antimicrobial Titanium Dioxide Nanotubes Obtained Through a Combination of Atomic Layer Deposition and Electrospinning Technologies. *J. Nanomater.*, 2018, **8** (128), P. 1–17.

[24] Chen N., Deng D., Li Y., Xing X., Xiao X., Wang Y. TiO_2 nanoparticles functionalized by Pd nanoparticles for gas-sensing application with enhanced butane response performances. *Sci. Rep.*, 2017, **7** (7692), P. 1–11.

[25] Kil H., Jung Y., Moon J., Song J., Lim D., Cho S. Glycothermal Synthesis and Photocatalytic Properties of Highly Crystallized Anatase TiO_2 Nanoparticles. *J. Nanosci. Nanotechnol.*, 2015, **15** (8), P. 6193–6200.

[26] Mosquera-Pretelt J., Mejia M.I., Marin J.M. Synthesis and Characterization of Photoactive S-TiO_2 from $TiOSO_4$ Precursor Using an Integrated Sol-Gel and Solvothermal Method at Low Temperatures. *J. Adv. Oxid. Technol.*, 2018, **21** (1).
[27] Mendoza-Anaya D., Salas P., Chavez C.A., Pérez-Hernández R. Microstructural characterization and morphology of TiO_2 for thermoluminescent applications. *Rev. Mex. Fis.*, 2003, **1** (50), P. 12–16.
[28] Dodoo-Arhin D., Buabeng F.P., Mwabora J.M., Amaniampong P.N., Agbe H., Nyankson E., Obada D.O., Asiedu N.Y. The effect of titanium dioxide synthesis technique and its photocatalytic degradation of organic dye pollutants. *Heliyon*, 2018, **4** (7).
[29] Dong F., Zhao W., Wu Z., Guo S. Band structure and visible light photocatalytic activity of multi-type nitrogen doped TiO_2 nanoparticles prepared by thermal decomposition. *J. Hazard. Mater.*, 2009, **162** (2–3), P. 763–770.
[30] Huang M., Xu C., Wu Z., Huang Y., Lin J., Wu J. Photocatalytic discolorization of methyl orange solution by Pt modified TiO_2 loaded on natural zeolite. *Dyes Pigm.*, 2008, **77** (2008), P. 327–334.
[31] Sing K.S.W., Everett D.H., Haul R.A.W., Moscou L., Pieroti R.A., Rouquerol J., Siemieniewska T. Reporting Physisorption Data for Gas/Solid Systems with Special Reference to the Determination of Surface Area and Porosity. *Pure & Appl. Chem.*, 1985, **57** (4), P. 603–619.
[32] Liu Y., Wang X., Yang F., Yang X. Excellent antimicrobial properties of mesoporous anatase TiO_2 and Ag/TiO_2 composite films. *Microporous Mesoporous Mater.*, 2008, **114** (1–3), P. 431–439.
[33] Naik K., Chatterjee A., Prakash H., Kowshik M. Mesoporous TiO_2 Nanoparticles Containing Ag Ion with Excellent Antimicrobial Activity at Remarkable Low Silver Concentrations. *J. Biomed. Nanotechnol.*, 2013, **9** (4), P. 664–673.
[34] Budi C.S., Kartini I., Rusdiarso B. Synthesis of mesoporous titania by potato starch templated sol-gel reactions and its characterization. *Indo. J. Chem.*, 2010, **10** (1), P. 26–31.
[35] Lan K., Wang R., Zhang W., Zhao Z., Elzatahry A., Zhang X., Liu Y., Al-Dhayan D., Xia Y., Zhao D. Mesoporous TiO_2 microspheres with precisely controlled crystallites and architectures. *Chem.*, 2018, **4** (10), P. 2436–2450.
[36] Pal A., Pehkonen S.O., Yu L.E., Ray M.B. Photocatalytic inactivation of Gram-positive and Gram-negative bacteria using fluorescent light. *J. Photochem. Photobiol. A*, 2007, **186** (2–3), P. 335–341.
[37] Liu Y., Zhu X., Yuan D., Wang W., Gao L. Preparation and characterization of TiO_2 based on wood templates. *Scientific Report*, 2020, **10**, 12444.
[38] Fu G., Vary P.S., Lin CT. Anatase TiO_2 Nanocomposites for antimicrobial coatings. *J. Phys. Chem. B*, 2005, 109 (18), P. 8889–8898.
[39] Alhadrami H.A., Baqasi A., Iqbal J., Shoudri R.A.M., Ashshi A.M., Azhar E.I., Al-Hazmi F., Al-Ghamdi A., Wageh S. Antibacterial Applications of Anatase TiO_2 Nanoparticle. *Am. J. Nanomater. (Print)*, 2017, **5** (1), P. 31–42.
[40] Valgas C., Machado de Souza S., Smânia E.F.A., Smânia Jr. A. Screening methods to determine antibacterial activity of natural products. *Braz. J. Microbiol.*, 2007, **38**, P. 369–380.
[41] Xing Y., Li X., Xu Q., Che Z., Li W., Bai Y., Li K. Effect of TiO_2 nanoparticles on the antibacterial and physical properties of polyethylene-based film. *Prog. Org. Coat.*, 2012, **73** (2–3), P. 219–224.
[42] Makowski A., Wardas W. Photocatalytic degradation of toxins secreted to water by cyanobacteria and unicellular algae and photocatalytic degradation of the cells of elected microorganisms. *Current Topics in Biophysics*, 2001, **25** (1), P. 19–25.

Submitted 15 November 2021; revised 14 June 2022; accepted 16 October 2022

Information about the authors:

L. Rohmawati – Physics Department, Faculty of Mathematics and Natural Science, Universitas Negeri Surabaya, Ketintang, Gayungan, Surabaya 60231, Indonesia; lydiarohmawati@unesa.ac.id

Istiqomah – Physics Department, Faculty of Mathematics and Natural Science, Universitas Negeri Malang, Semarang 5, Malang 65145, Indonesia; istiqomahistiqomah1999@gmail.com

A. A. Pratama – Physics Department, Faculty of Mathematics and Natural Science, Universitas Negeri Surabaya, Ketintang, Gayungan, Surabaya 60231, Indonesia; angela.17030224011@mhs.unesa.ac.id

W. Setyarsih – Physics Department, Faculty of Mathematics and Natural Science, Universitas Negeri Surabaya, Ketintang, Gayungan, Surabaya 60231, Indonesia; worosetyarsih@unesa.ac.id

N. P. Putri – Physics Department, Faculty of Mathematics and Natural Science, Universitas Negeri Surabaya, Ketintang, Gayungan, Surabaya 60231, Indonesia; nugrahaniprimary@unesa.ac.id

Munasir – Physics Department, Faculty of Mathematics and Natural Science, Universitas Negeri Surabaya, Ketintang, Gayungan, Surabaya 60231, Indonesia; munasir_physics@unesa.ac.id

Darminto – Physics Department, Faculty of Science and Data Analytics, Institut Teknologi Sepuluh Nopember (ITS), Keputih, Sukolilo, Surabaya 60111, Indonesia; darminto@physics.its.ac.id

Conflict of interest: the authors declare no conflict of interest.